Constraining many ALPs with Terrestrial Experiments

Based on: arxiv.org/TBD with A. de Giorgi, J. Jaeckel, S.M., V. Takhistov

Sebastian Monath

16.12.2025 Saragossa

Motivation

Let's state the obvious: The axion is a promising solution to the CP problem

$$\mathcal{L} = \sum_q \bar{q}(i\not{D} - m_q e^{i\theta_q \gamma})q - \frac{1}{4} G^a_{\mu\nu} G^{a\mu\nu} + (\theta + \frac{a}{f_a}) \frac{g_s^2}{32\pi^2} G^a_{\mu\nu} \tilde{G}^{a\mu\nu}$$

Induces effective potential for axion:

$$E(\theta) = -2Ke^{-8\pi^2/g_s^2} \cos(\theta + \theta_q + \frac{a}{f_a})$$

$\rightarrow$ Dynamical CP-solution

The QCD Axion Band

Chiral Lagrangian techniques give prediction for axion mass and photon-coupling:

$$m_a^2 = \frac{m_u m_d}{(m_u^2 + m_d^2)} \frac{m_\pi^2 f_\pi^2}{f_a^2} \approx 5.7 \left(\frac{10^{12}\ \text{GeV}}{f_a} \right)$$

$$g_{a\gamma\gamma} = \frac{\alpha}{2\pi f_a} \left(\frac{E}{N} - \left(\frac{2}{3} \frac{4m_d + m_u}{m_u + m_d} \right) \right)$$

$\rightarrow$ In standard axion constructions the mass-coupling ratio is well constrained

The QCD Axion Band

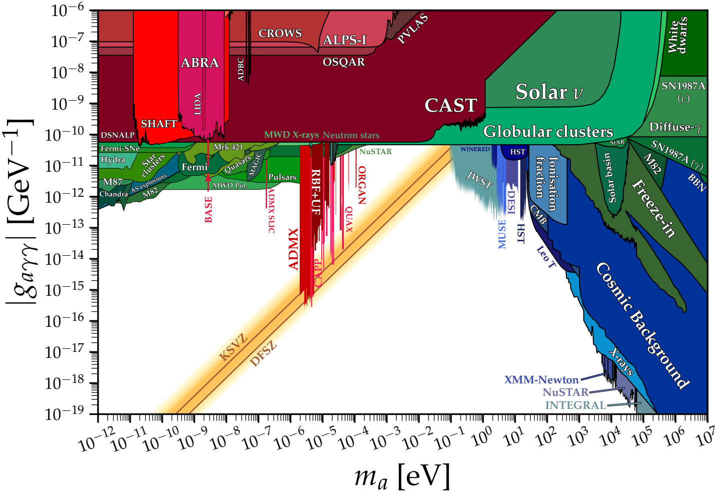

QCD Axion Band and Limits [Hare, Git]

Thinking outside the QCD axion band

We distinguish two cases:

- → String Theory inspired: Plethora of ALPs across scales, a single one in the QCD band
- → Multiple pseudoscalars contributing to Peccei-Quinn, entirely located outside of QCD band

[Gavela et al., 2024]: General Lagrangian of light pseudoscalars:

$$\mathcal{L} = \sum_{i=1}^{N}\left(\frac{1}{2}\partial^{\mu}a_i\partial_{\mu}a_i - \frac{m_i^2}{2}a_i^2\right) - \frac{1}{4}F_{\mu\nu}F^{\mu\nu} - \frac{g_{a\gamma\gamma}}{4}(\sum_{i=1}^{N}c_i a_i F_{\mu\nu}\tilde{F}^{\mu\nu})$$

Satisfying sum rule:

$$1 = \sum_{i=1}^{N}\frac{1}{g_i} \equiv \sum_{i=1}^{N}\frac{m_{\text{eff}}^2 f_i^2}{\chi_{\text{QCD}}}$$

Multiple ALPs in Laboratory Experiments

Models outside usual QCD axion band are well motivated $\rightarrow$ Need to understand axion phenomenology of representative models (Neglecting electron couplings)

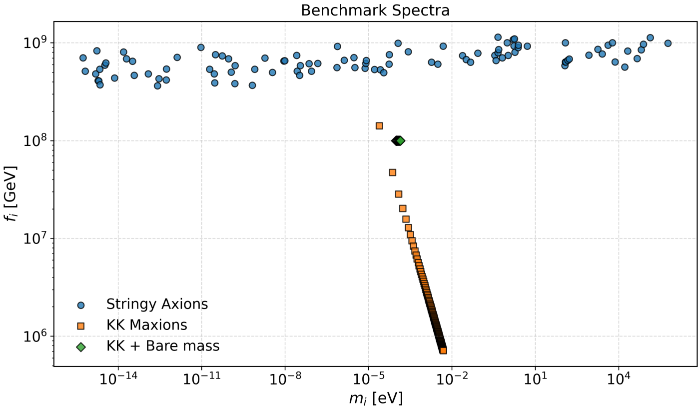

Structure

- → Examples of UV origins of benchmark patters
- → Pheno Constraints
  - → LSW
  - → Helioscopes
  - → A comment on Haloscopes

String Inspired Model

Standard Consideration $\rightarrow$ Pseudoscalar generated by Instanton effects on cycles of area $A \approx L^2$ of 10d Manifold[Arvanitaki et al., 2010]:

$$\mathcal{L} = \frac{f_a^2}{2}(\partial a)^2 - \Lambda^4 U(a)$$

so that $m = \frac{\Lambda^2}{f_a}$

$$\Lambda^4 = \mu^4 \exp(-S)$$

With the estimate:

$$f_a \approx \frac{M_{\text{Pl}}}{S}$$

$\rightarrow$ Assuming uniform distribution of actions

- Uniform distribution of decay constants $f_a = \frac{M_{\text{Pl}}}{S}$
- Log distribution of masses $m = \mu^2 \exp\left(-S/2\right)/f_a$

Extra Dimensional Model

Simple way to realize non-canonical coupling-mass patterns [De Giorgi and Ramos, 2025]: QCD on higher dimensional manifold $\mathcal{M}$:

$$S = \int_{\mathbb{R}^4} \int_{\mathcal{M}} \sqrt{g} \left[\frac{M^\delta}{2} g^{AB} \partial_A a(x,y) \partial_B a(x,y) + \frac{\alpha_s}{8\pi} \frac{a(x,y)}{f_d} G^{\mu\nu} \tilde{G}_{\mu\nu} \delta_{\text{4d-sub}}(y) \right]$$

Integrate out finite dimension:

$$\mathcal{L} = \sum_n \left(\frac{1}{2} (\partial_\mu a)^2 - \frac{1}{2} \mu_n^2 a_n^2 \right) + \frac{1}{f_4} \frac{\alpha_s}{8\pi} \alpha_n \psi^n_{\text{4d-sub}} G^{\mu\nu} \tilde{G}_{\mu\nu}$$

for extra dimensions of size $2\pi R$ and dimension $4 + \delta$

$$a(x,y) = \frac{1}{(2\pi R M)^{\frac{\delta}{2}}} \sum_n a_n(x) \psi_n(y)$$

Extra Dimensional Model

Sufficient for qualitative features: 5d model with flat metric

$$f_4 = \sqrt{2\pi RM} f_d$$
$$\mu_n = \frac{n}{R}$$
$$\psi_n(y) = \cos(\mu_n y) \begin{cases} 1 & \text{for } n = 0 \\ (-1)^n \sqrt{2} & \text{for } n > 0 \end{cases}$$

Parameter $y = \frac{\mu_1}{\sqrt{\chi_{\text{QCD}}}} f_4$ determines spectrum

$$m_n = \frac{\sqrt{\chi_{\text{QCD}}}}{f_4} y(n + \frac{1}{2})$$
$$f_n = f_4 \begin{cases} \frac{\sqrt{2}\pi^2}{y^2(1+2n)} & \text{for } \mu_n \ll m_{\text{PQ}} \\ 1/\psi_1 & \text{for } \mu_n > m_{\text{PQ}} \end{cases}$$

Extra Dimensional Model

Parameter $y = \frac{\mu_1}{\sqrt{\chi_{\rm QCD}}} f_4$ determines spectrum

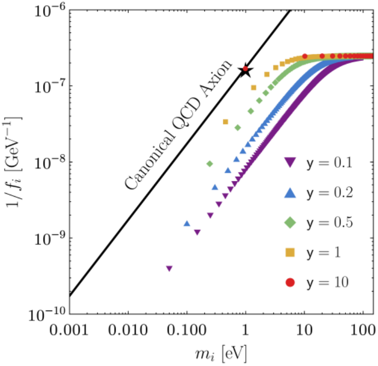

Figure: KK-Axion distribution for different y-Parameters. De Giorgi, Ramos 2024 [De Giorgi and Ramos, 2025]

One more generalization

If we do not insist that our multidimensional pseudoscalar solves CP $\rightarrow$
One more pattern becomes viable
Include tree-level mass

$$S = \int_{\mathbb{R}^4} \int_{\mathcal{M}} \sqrt{g} \Big(\frac{M^\delta}{2} g^{AB} \partial_A a(x,y) \partial_B a(x,y) + \frac{m_0^2}{2} a(x,y)^2 + \frac{\alpha_s}{8\pi} \frac{a(x,y)}{f_d} G^{\mu\nu} \tilde{G}_{\mu\nu} \delta_{\text{4d-sub}}(y) \Big)$$

We find:

- $\longrightarrow$ $m_n = \sqrt{m_0^2 + (\frac{n}{R})^2}$
- $\longrightarrow$ $f_n = \text{const}$ (for large m_0)

Light shining through walls

Effective theory for ALPs and QED:

$$\mathcal{L} = \sum_{n=1}^{N} \left(\frac{1}{2} \partial^{\mu} a_n \partial_{\mu} a_n - \frac{1}{2} m_n^2 a_n^2 \right) - \frac{1}{4} F^{\mu\nu} F_{\mu\nu} - \frac{g_{a\gamma}}{4} \left(\sum_{n=1}^{N} c_n a_n \right) F^{\mu\nu} \tilde{F}_{\mu\nu}$$

Quantity of interest: Abs. Sq of Photon Field Amplitude at detector behind wall

$\rightarrow$ Can be treated in classical field theory

Sketch of calculation

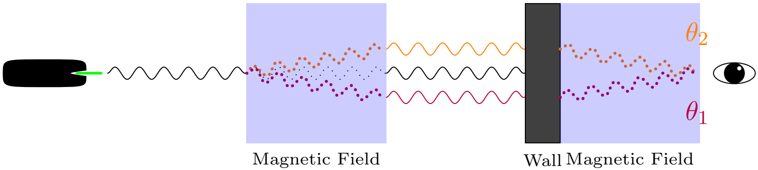

Sketch of propagation of different ALP contributions to photon amplitude

Coherence effects

$$P = \Bigg[\sum_{n=1} P_{\gamma\to n}(L_1) P_{\gamma\to n}(L_2) \\ + 2 \sum_{k<n} \Pi^{\star}_{1,k}\Pi^{\star}_{2,k}\Pi_{1,n}\Pi_{2,n} \cos\left(\frac{m_n^2 - m_k^2}{2\omega} \left(\frac{L_1 + L_2}{2} + L_w \right) \right) \Bigg]$$

with:

$$\Pi_n(L) \approx \frac{2\omega\beta_n}{m_n^2} \sin\left(\frac{m_n^2 L_a}{4\omega} \right), \qquad P^2_{\gamma\to n} \approx \Pi_n(L)^2,$$

- → Destructive interference possible
- → Degenerate masses: Signal scales with N^2
- → Explicit dependence on wall

Reminder of benchmark models

Model:	Axiverse-Inspired	KK-Maxion-Inspired	KK-ALP-Inspired
m_n	$\sim \mu^2 e^{-S/2}/f_n$	$\left(n-\frac{1}{2}\right)\mu_1$	$\sqrt{m_0^2+(n\mu_1)^2}$
f_n	$\sim \Lambda/S$	$f_a \times \frac{\sqrt{2}}{2n-1}\left(\frac{\pi m_a}{\mu_1}\right)^2$	$f_a = \text{const.}$
Values (LSW):	$\begin{cases}\mu = \bar{M}_P, \\ \Lambda = 10^{11}\text{ GeV}, \\ S \in [100, 200]\end{cases}$	$\begin{cases}\mu_1 = 5\times10^{-5}\text{ eV}, \\ m_a = \mu_1/\pi, \\ f_a = 10^8\text{ GeV},\end{cases}$	$\begin{cases}\mu_1 = 10^{-6}\text{ eV}, \\ m_0 = 10^{-4}\text{ eV}, \\ f_a = 10^8\text{ GeV},\end{cases}$

Summary of the benchmark models adopted in this work to showcase the results.

Reminder of benchmark models

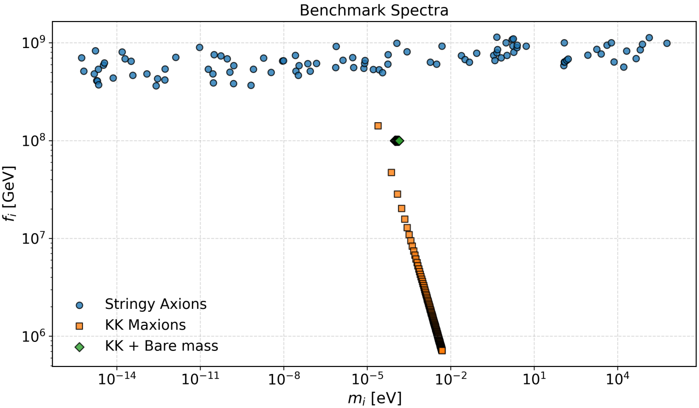

Benchmark Model

LSW Signatures of Benchmark Models

$\propto \beta_n^4 L^4$

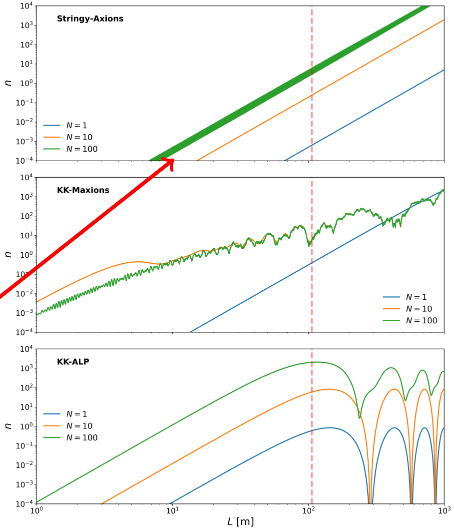

Conclusions

- → Varying L_w straightforward way to distinguish multi- from single ALP hypotheses
- → Stringy models: Low masses $\rightarrow$ always beneficial to increase L
- → Maxion models: Lowest mass contribution eventually dominates
- → Degenerate KK-models: Coherent enhancement as generic feature

Localising the masses

Upon first detection: L_w can be scanned over to find contributing modes

$$\mathcal{F}_{L_w}\left[\cos(2(x_i - x_j)(L + L_w)\right](k) =$$
$$\sqrt{\frac{\pi}{8}}\left[e^{2iLx_{ij}}\delta(k + 2x_{ij}) + e^{-2iLx_{ij}}\delta(k - 2x_{ij})\right].$$

Individual modes of $x_{ij} \approx \frac{\Delta m_{ij}^2}{4\omega} \approx 1.3 \times 10^6[\mathrm{m}^{-1}] \times \left(\frac{\mathrm{eV}}{\omega}\right)\left(\frac{m_n}{\mathrm{eV}}\right)^2$ $\mathcal{O}(10)$ for benchmark considered here

Experimental optimism

For sufficiently high sample rate w.r.t. oscillation length $\frac{2\pi\omega}{\Delta m_{ij}^2}$

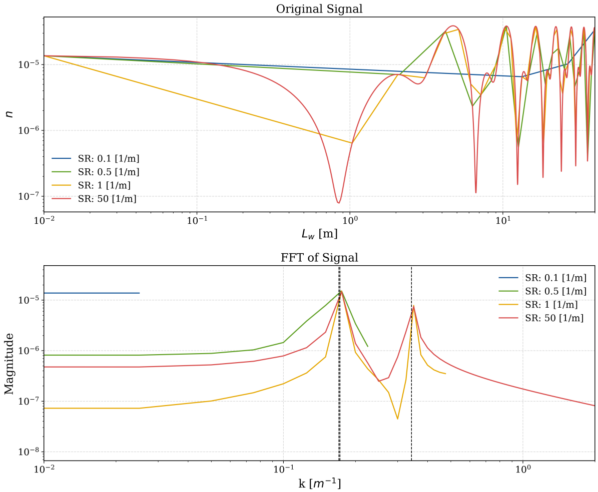

Helioscope Theory

Individual wave packets produced predominantly in solar core, converted in magnetic field on earth

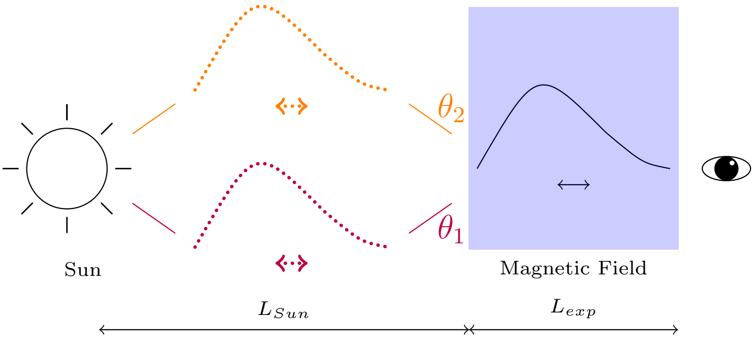

Sketch of propagation of different ALP wave packets upon conversion to photon wave packet

"Subtleties"

1. Coherence effects: Each wave packet picks up phase:

$$\theta \approx \left(L_{\mathrm{Sun}} + \frac{L_{\mathrm{mag}}}{2} \right) \frac{m_i^2 - m_j^2}{2\omega}$$

Experimentally, we (normally) measure the integrated signal $\rightarrow$ coherence effects for $\Delta m_{ij}^2 \sim< (\frac{\Delta L_{sun}}{\omega} + L\frac{\Delta\omega_{\mathrm{Spec}}}{\omega}) \approx 10^{-12}$ eV Numerically reliable approximation: Take Cos in coherent part to 1 if $\frac{\Delta m_{ij}^2 L}{4\omega} < 2\pi$
Otherwise neglect

"Subtleties"

2. Medium effects: Effective theory for keV photon in medium → include complex dispersion relation

$$\omega^2 - k^2 = m_\gamma^2 + i\omega\Gamma$$

Otherwise approach remains the same

Positive "Photon Mass" for solar energies → Resonances appear

$$P_{a_n \to \gamma} \approx \left(\frac{\beta_n}{2}\right)^2 \frac{1 - 2e^{\frac{-\Gamma L}{2}} \cos(q_n L) + e^{-\Gamma L}}{q_n^2 + \Gamma^2/4}$$

Experimental opportunities

In helioscopes no variable wall size to immediately distringuish multi-ALP signals
Therefore: Additional experimental parameters $\rightarrow$ the analytical behavior of non-coherent part can be determined

- $\longrightarrow$ ^{4}He pressure in bores (Haloscope-like scanning)
- $\longrightarrow$ Photon energy ω using monochromators
- $\longrightarrow$ (Regeneration length L)

Reminder of benchmark models

Model:	Axiverse-Inspired	KK-Maxion-Inspired	KK-ALP-Inspired
m_n f_n	$\sim \mu^2 e^{-S/2}/f_n$ $\sim \Lambda/S$	$\left(n - \frac{1}{2}\right)\mu_1$ $f_a \times \frac{\sqrt{2}}{2n-1}\left(\frac{\pi m_a}{\mu_1}\right)^2$	$\sqrt{m_0^2 + (n\mu_1)^2}$ $f_a = \text{const.}$
Values (LSW):	$\begin{cases} \mu = \bar{M}_P, \\ \Lambda = 10^{11}\ \text{GeV}, \\ S \in [100, 200] \end{cases}$	$\begin{cases} \mu_1 = 5 \times 10^{-5}\ \text{eV}, \\ m_a = \mu_1/\pi, \\ f_a = 10^8\ \text{GeV}, \end{cases}$	$\begin{cases} \mu_1 = 10^{-6}\ \text{eV}, \\ m_0 = 10^{-4}\ \text{eV}, \\ f_a = 10^8\ \text{GeV}, \end{cases}$
Values (helioscopes):	$\begin{cases} \mu = \bar{M}_P, \\ \Lambda = 10^{11}\ \text{GeV}, \\ S \in [100, 200] \end{cases}$	$\begin{cases} \mu_1 = 5 \times 10^{-3}\ \text{eV}, \\ m_a = \mu_1/\pi, \\ f_a = 10^{8.5}\ \text{GeV}, \end{cases}$	$\begin{cases} \mu_1 = 10^{-4}\ \text{eV}, \\ m_0 = 10^{-2}\ \text{eV}, \\ f_a = 10^8\ \text{GeV}, \end{cases}$

Summary of the benchmark models adopted in this work to showcase the results.

Varying the gas pressure

→ Each particle pops up as resonance

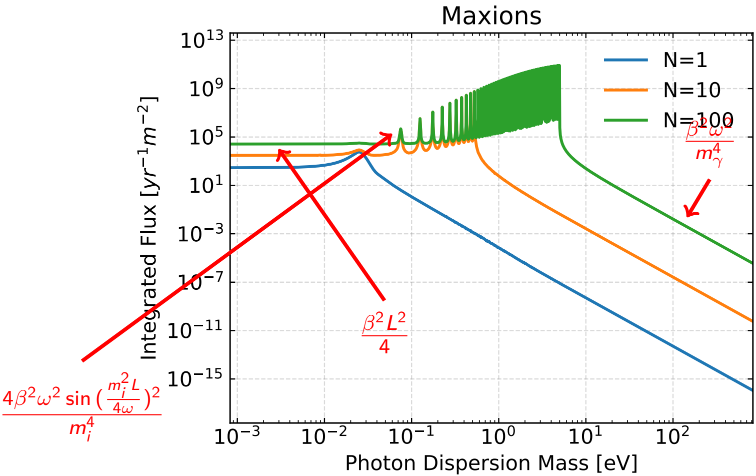

Singling Out a Frequency

→ Emission spectrum modulated by detection probabiltiy

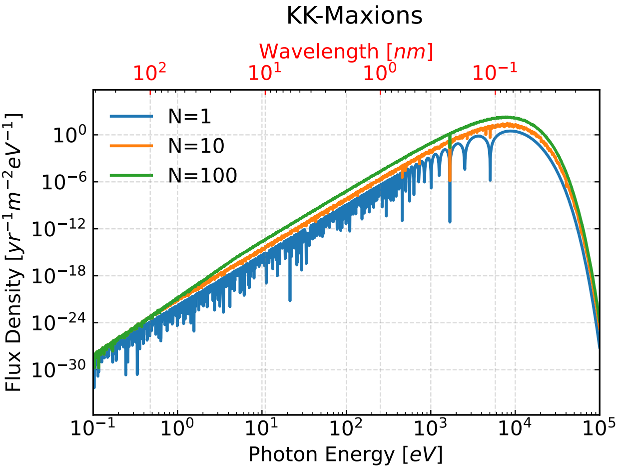

Varying the Regeneration Length

→ Max Signal $\propto m^{-4}$ c.f. m^{-8} for LSW → lowest one no longer dominates

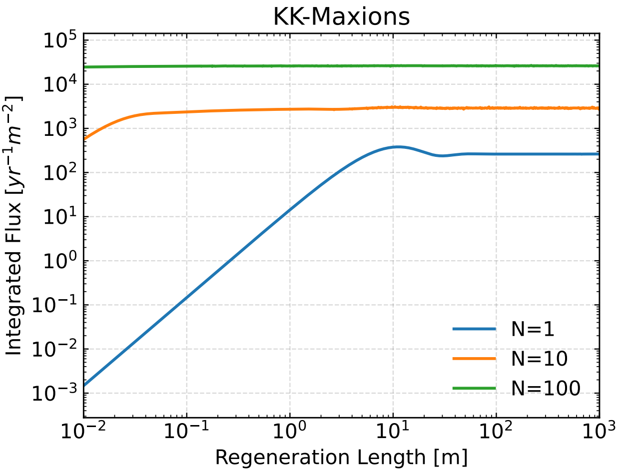

Conclusions

- → Distinction of multi-/single-ALP models not as straightforward as in LSW models
- → More (and perhaps more convenient) experimental parameters to vary
- → Shift in contribution of the individual ALPs in benchmark sets (more massive ones have proportionally larger contribution)
- → Coherence effects only relevant in very limited mass (difference) range → here only stringy models

Summary

→ Investigated qualitative behavior of laboratory bounds for different characteristic patterns of multi-ALP models

→ Discussed the role of coherence effects

→ Proposed ways to explicitly determine ALP parameter sets
$\rightarrow$ pointed out in particular capacity of LSW experiments to distinguish multi-ALP from single ALP models

$$
\begin{aligned}
f_a &\approx \frac{M_{\mathrm{Pl}}}{S} \\
M_{\mathrm{Pl}} &\approx g_s^{-2} L^6 l_S^{-8} \\
f_a^2 &\approx L^6 l_s^{-4} A^{-2} \approx L^2 l_s^{-4} \\
S &\approx g_s^{-1} l_s^{-2} L^2
\end{aligned}
$$

Varying the gas pressure

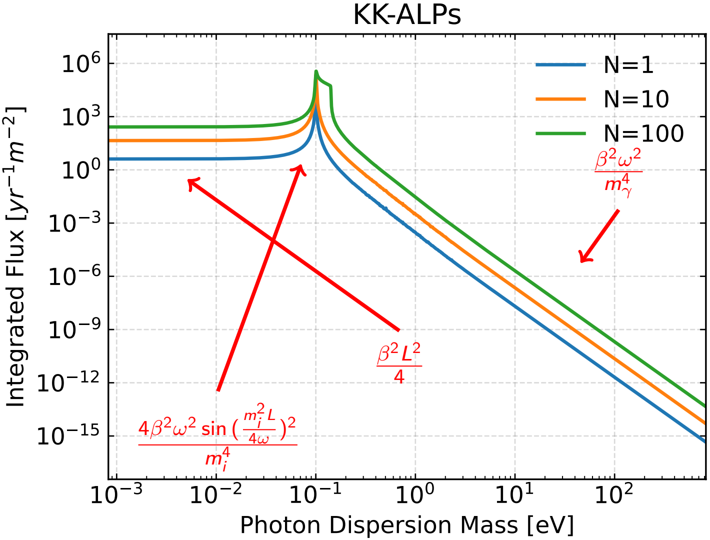

Varying the gas pressure

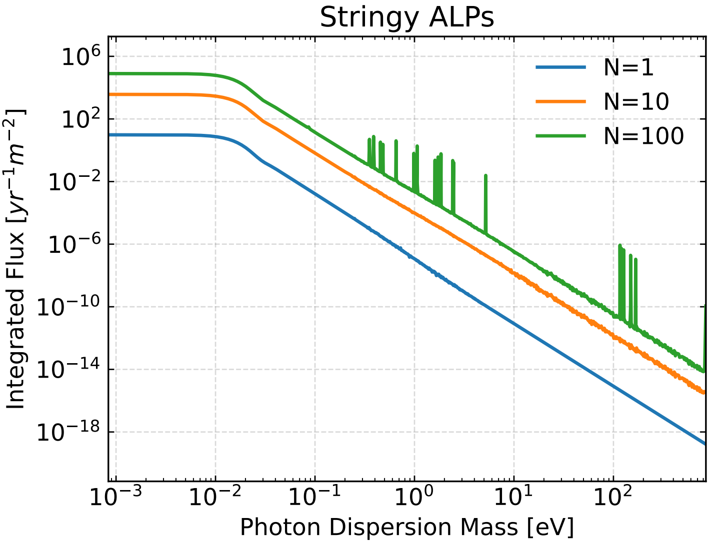

Singling Out a Frequency

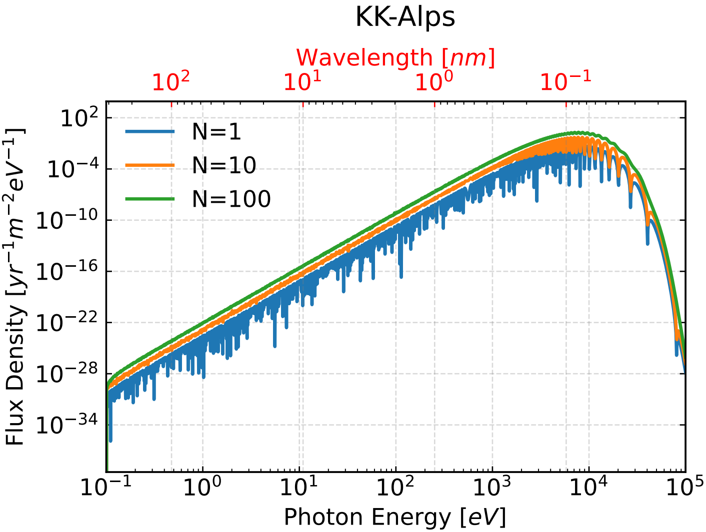

Singling Out a Frequency

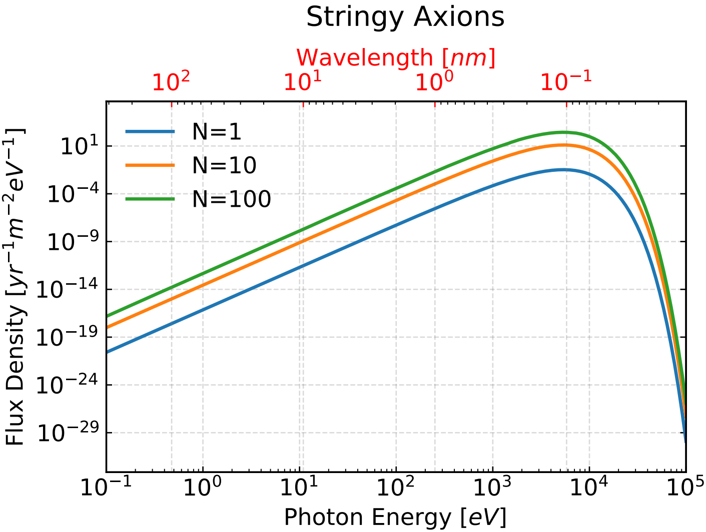

Varying the Regeneration Length

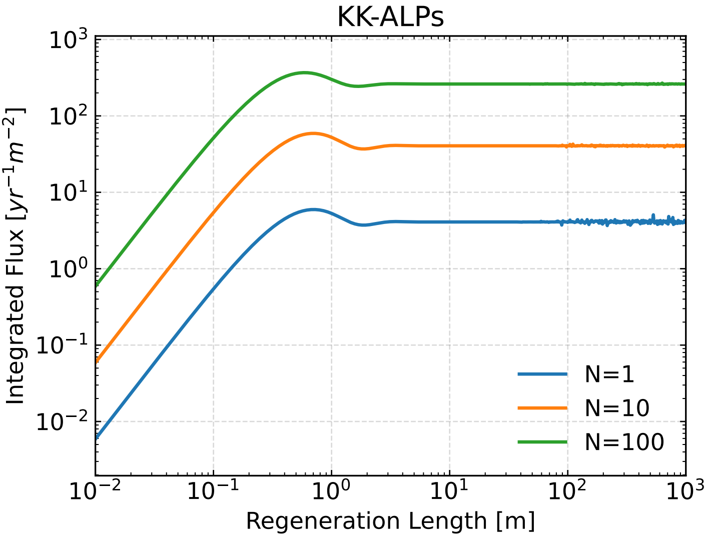

Varying the Regeneration Length

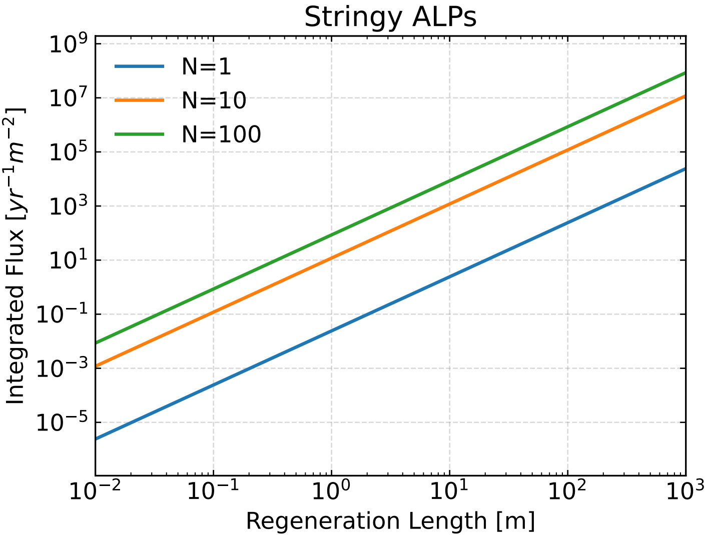

A Comment on Haloscopes

Upside: Straightforward way to find the exact masses of all accessible ALPs (c.f. pressure scanning in helioscopes)
However: Signal-to-noise ratio in Haloscope experiments

$$\mathrm{SNR}_n \propto g^2_{a_n\gamma}\rho_n$$

$\longrightarrow$ Degeneracy between abundance and coupling fancyarrow determining coupling requires complementary experiments
Although:

$$\frac{\mathrm{SNR}_n}{\mathrm{SNR}_m} = \frac{g_{a_n\gamma}\rho_n}{g_{a_m\gamma}\rho_m}$$

Can be constrained by cosmological arguments

References I

Arvanitaki, A., Dimopoulos, S., Dubovsky, S., Kaloper, N., and March-Russell, J. (2010).
String axiverse.
Physical Review D—Particles, Fields, Gravitation, and Cosmology, 81(12):123530.

De Giorgi, A. and Ramos, M. (2025).
Extra-dimensional axion patterns.
Physical Review D, 111(7):075006.

Gavela, B., Quílez, P., and Ramos, M. (2024).
The qcd axion sum rule.
Journal of High Energy Physics, 2024(4):1–28.

References II

Hare, C. (Git).
Axion limits.
https://github.com/cajohare/AxionLimits.